HHS Public Access

Author manuscript

Spine J. Author manuscript; available in PMC 2023 April 01.

Published in final edited form as:

Spine J. 2022 April ; 22(4): 677–689. doi:10.1016/j.spinee.2021.10.014.

Heterogeneous macrophages contribute to the pathology of disc herniation induced radiculopathy

Li Jin[1], **Li Xiao**[1], **Mengmeng Ding**[1,2], **Aixing Pan**[1,3], **Gary Balian**[1,4], **Sun-Sang J Sung**[5], **Xudong Joshua Li**[1,6,*]

[1]Department of Orthopaedic Surgery, University of Virginia, Charlottesville, VA 22908, USA

[2]Current address: Department of Anesthesiology, Shengjing hospital, China Medical University, Shenyang, China

[3]Current address: Department of Orthopaedic Surgery, Chaoyang Hospital, Capital Medical School, Beijing, China

[4]Department of Biochemistry and Molecular Genetics, University of Virginia, Charlottesville, VA 22908.

[5]Department of Medicine and Center for Immunity, Inflammation, and Regenerative Medicine, University of Virginia, Charlottesville, VA 22908, USA

[6]Department of Biomedical Engineering, University of Virginia, Charlottesville, VA 22904, USA

Abstract

Background context: Macrophages play important roles in the progression of intervertebral disc herniation and radiculopathy.

Purpose: To better understand the roles of macrophages in this process, we developed a new mouse model that mimics human radiculopathy.

Study Design/Setting: A preclinical randomized animal study.

Methods: Three types of surgeries were performed in randomly assigned Balb/c mice. These were spinal nerve exposure, traditional anterior disc puncture, and lateral disc puncture with nerve exposure (n=16/group). For the nerve exposure group, the left L5 spinal nerve was exposed without disc injury. For the traditional anterior puncture, L5/6 disc was punctured by an anterior approach as previously established. For lateral puncture with nerve exposure, the left L5 spinal nerve was exposed by removing the psoas major muscle fibers, and the L5/6 disc was punctured laterally on the left side with a 30G needle, allowing the nucleus to protrude toward the L5

[*]**Correspondence:** Xudong Joshua Li, xl2n@virginia.edu, Phone: 434-924-5937, Address: Department of Orthopaedic Surgery, University of Virginia, Charlottesville, VA 22908, USA.

Conflict of Interest

The authors declare that the research was conducted in the absence of any commercial or financial relationships that could be construed as a potential conflict of interest.

spinal nerve. Mechanical hyperalgesia (pain sensitivity) of hind paws was assessed with electronic von Frey assay on alternative day for up to 2 weeks. MRI, histology, and immunostaining were performed to confirm disc herniation and inflammation.

Results: Ipsilateral pain in the lateral puncture with nerve exposure group was significantly greater than the other groups. Pro-inflammatory cytokines IL-1β and IL-6 were markedly elevated at the hernia sites of both puncture groups and the spinal nerve of lateral puncture with never exposure group on postoperative day 7. Heterogeneous populations of macrophages were detected in the infiltration tissue of this mouse model and in tissue from patients undergone discectomy.

Conclusions: We have established a new mouse model that mimics human radiculopathy and demonstrates that a mixed phenotype of macrophages contribute to the pathogenesis of acute discogenic radiculopathy.

Clinical significance: This study provides a clinically relevant *in vivo* animal model to elucidate complex interactions of disc herniation and radicular pain, which may present opportunities for the development of macrophage-anchored therapeutics to manage radiculopathy.

Keywords

low back pain; radiculopathy; disc herniation; inflammation; macrophages; animal model

Introduction

Low back and radicular pain are the leading causes of disability worldwide with a lifetime prevalence of 80% and expenditures greater than $100 billion in the US [1–3]. Intervertebral disc (IVD) herniation is the most common cause of back and radicular pain [4,5]. The herniated disc tissue protrudes toward the adjacent nerve and stimulates inflammatory responses that cause neurologic symptoms. Despite tremendous progress in disc research, the pathophysiology and the underlying cellular mechanisms are still elusive because of the complex nature of the disease.

Cervical radiculopathy and lumbar radiculopathy are traditionally thought to be due to the nerve root compression aroused by the herniated disc. However, the severity of clinical symptoms, such as paresis, muscle weakness, impaired reflexes, and sensory deficits, do not always correlate with the size of disc hernia [6], suggesting nerve pinching is not the only cause of pain. Indeed, recent experimental findings suggested that inflammatory mediators play critical roles in disease pathogenesis [7–9]. The normal IVD is an immune-privileged organ composed of the inner nucleus pulposus (NP) and the outer annulus fibrosus (AF). The jelly-like NP is composed of NP cells, type II collagen and proteoglycans. The AF region is composed of AF cells, type I and type II collagen fibers arranged in concentric layers. When discs wear out, the AF cracks and the NP herniates out, which is recognized as a foreign body by our immune system. Immune cells infiltrate the disc hernia and evoke a cascade of events, such as cytokine production by both disc cells and immune cells, exacerbating the inflammation and pain [7,8,10,11].

Macrophages are highly plastic phagocytic cells that mediate both the initiation and resolution of inflammation, and they exhibit various phenotypes reflecting a spectrum of

activation states in response to local environment. Macrophages are traditionally designated as classically activated (M1-like) and alternatively activated (M2-like) macrophages [12,13]. M1-like macrophages have anti-microbial and anti- tumor activities and mediate ROS-induced tissue damage, which impair tissue regeneration and wound healing. M2-like macrophages (M2a, M2b, M2c, M2d) protect against such tissue damage and inhibit the chronic inflammatory response, given their capacity in phagocytosis, scavenging debris and apoptotic cells, and promoting tissue repair and wound healing [14,15]. Several studies suggested that proinflammatory macrophages increase following disc herniation [16–19]. Using a bone marrow GFP chimera mouse model, Kawakubo et al showed that the proportion of GFP^+ macrophages and $CD86^+$ GFP^+ macrophages increased following disc herniation and its proportion was significantly higher than that in GFP^- macrophages, suggesting the recruitment of macrophages in the hernia sites polarized to proinflammatory macrophages following disc herniation [20]. Using immunohistochemistry, Nakazawa et al showed that $CCR7^+$ and $CD163^+$ macrophages significantly increased in severe degenerative human cadaveric disc tissues. Abundant infiltration of $CD68^+$ $CD33^-$ cells, with variable levels of CD11b, CD11c, and CD40, was also observed in herniated discs of human samples [10]. A recent study of canine disc herniation samples also showed a mixed phenotype of macrophages, both proinflammatory and anti-inflammatory phenotypes [21]. These findings suggest the importance of understanding the immunophenotype of inflammatory responses and cellular mechanisms in uncovering the pathology of disc herniation. However, the roles and phenotypes of macrophages in the pathogenesis of disc herniation and radiculopathy remain unclear.

To address this problem, establishing an animal model that simulates the pathology of human radiculopathy is a prerequisite. In patients suffering from disc herniation, the dorsal root ganglion (DRG) or nerve roots are typically exposed to the ruptured disc tissues, which induced radicular pain and cascades of inflammation [22,23]. To this end, we aim to establish a mouse model of radiculopathy mimicking human conditions and to characterize phenotypes and roles of macrophages at disc hernia sites. Results from this study will provide a clinically relevant *in vivo* model to elucidate complex interactions in the niche of disc herniation and radicular pain, which may present opportunities for the development of macrophage-anchored therapeutics to manage radiculopathy.

Materials and Methods

Animals

The use of animals was approved by our Institutional Animal Care and Use Committee. Balb/c mice (10–12 week, male, 20–25g, Envigo) were socially housed at the centralized animal experiments facility. The rooms were fitted with a 12-hour light/dark cycle and temperature of 25 °C. Food and water were provided ad libitum. A total of 48 mice were randomly assigned into three groups (n=16/group): spinal nerve exposure, traditional anterior disc puncture, and lateral disc puncture with spinal nerve exposure. An additional 10 mice were used randomly for sham surgery (n=4, same surgical procedure without disc puncture) or anterior disc puncture at L5/6 (n=6), and inflammatory infiltration tissues (~

1–2 mm granular yellowish tissue) were dissected on postoperative day (POD) 6 to analyze macrophage phenotypes.

Surgical procedures to model disc herniation induced radiculopathy

General anesthesia was performed by intraperitoneal injection of Ketamine/Xylazine (60–80/5–10mg/kg). The anatomic relationship of lumbar spinal nerve to IVD is shown in Fig. 1a–1b. Using aseptic techniques and a surgical microscope, mouse spines were exposed through an anterior midline trans-peritoneal approach. For all groups, after separating the peritoneum, L5 vertebral bodies were first identified. For the nerve exposure group, the left psoas major muscle fibers superficial to the L5 spinal nerve were removed without exposure of discs. For the traditional anterior disc puncture group, L5/6 disc was punctured with a 30G needle (Becton Dickinson, NJ) to ensure herniation of NP material in the mid-sagittal plane as we previously established [24]. For the lateral disc puncture with nerve exposure group, the left psoas major muscle fibers superficial to the L5 spinal nerve were first removed, then both left L5 nerve and L5/6 disc were exposed (Fig. 1b–1d), followed by lateral puncture of L5/6 disc at the left side using a 30 G needle to enable NP protrusion towards the exposed adjacent spinal nerves, as shown in the X-ray image (Fig 1e, red arrow indicates needle entry at the L5/6 disc). The granular inflammatory disc tissues were visualized in the disc puncture with nerve exposure group under a surgical microscope (Fig. 1f).

Magnetic Resonance Imaging (MRI)

MRI was performed at 2 weeks after surgery as previously described [25]. Under anesthesia, imaging was acquired using a 7T ClinScan Bruker MRI scanner. T2-weighted sections in the sagittal plane were obtained as a series of multiple two-dimensional slices.

Mechanical hyperalgesia (pain sensitivity)

Mechanical hyperalgesia was measured on both hind paws every other day post-surgery for up to 16 days. Paw withdrawal threshold was determined using an electronic Von Frey Anesthesiometer (IITC Life science, CA) per our established protocol [26–28]. Baseline data were collected for three consecutive days prior to surgery. Animals were acclimated to noise and temperature-controlled environments for at least one hour prior to testing. A rigid instrument tip was slowly raised to stimulate the middle of the hind paw until a nociceptive reaction was observed. Each hind paw was tested 5 times with a 1-minute interval, and the average of the 3 values deviating least from the median was calculated. Mechanical thresholds were presented as mean ± SEM at each time point. A single experienced operator performed all testing at the same time frame of a day.

Safranin-O staining of mouse spine sections

Mice were euthanized using CO_2 asphyxiation, followed by cervical dislocation on POD 3 and 7 (n=3 per time point per group). Lumbar spines were fixed with 10% neutral formalin, followed by decalcification in 0.25M EDTA for one week. Axial sections (5 μm thickness) were stained with Safranin-O and Fast Green to evaluate the severity of disc herniation,

such as cellularity, collagen fiber alignment, and loss of glycosaminoglycan as described previously [29–31].

Human surgical samples

With IRB approval, human inflammatory disc tissues were collected from surgical wastes during discectomy on four patients. Inflamed disc tissues were surgically dissected from the patients 3–6 month after disease onset. Samples were transported on ice and fixed in periodate-lysine- *p*-formaldehyde (PLP) fixture and processed for immunofluorescence staining.

Immunohistochemistry and analysis

Immunohistochemistry was performed as described previously [24,26]. Spine axial tissue sections (5 μm) were stained with antibodies for IL1-β (H-133, Santa Cruz Biotechnology 1:100), IL-6 (ab6672, Abcam 1:800), Ionized calcium binding adaptor molecule 1 (Iba-1, NB100–1028, Novus Biologicals; 1:200), or glial fibrillary acidic protein (GFAP, NB300–141, Novus Biologicals, 1:5000). Rabbit IgG was used as a negative control following identical procedures but excluding the primary antibody (Supplementary Figure. 1). Images were captured using a Nikon Eclipse E600 microscope. The same color hue settings were used throughout quantification using NIS element BR imaging software. Several square ROIs (region of interest), with a linear length of 150 μm that adequately represent the entire quantifiable cell area, were used and analyzed individually. A previously optimized object count threshold was loaded and maintained throughout the procedure for quantification of intensity. The average signal intensity was obtained by combing data from three mice with three to five sections each.

Immunofluorescence staining and analysis

For immunofluorescence staining, dissected inflammatory tissues were fixed in PLP fixative for 3h [32] After equilibration in 5% sucrose in 50 mM phosphate buffer (pH7 4) overnight, 2h in 15% sucrose, and 4h in 30% sucrose, the tissues were embedded in Optimal Cutting Temperature compound. Frozen tissue sections (5 μm) were permeabilized with 0.3% triton X-100, blocked with anti-FcγRII/FcγRIII mAb (clone 2 4G2) and serum, and stained with fluorochrome-conjugated antibodies [33,34]. Monoclonal antibodies from Biolegend were: A647-conjugated anti-CD11b (M1/70); A647-conjugated anti-F4/80 (BM8); FITC-anti-CD80 (W17149D), and anti-NOS2 (5C1B52). Rabbit-anti-CD68 (2449D), goat-anti MMR antibody (AF2535), and goat-anti CD163 antibody (AF1607) were from R&D system. Anti-MMR antibody was conjugated with an AlexaFluor antibody labeling kits (Invitrogen, Grand Island, NY) before cell staining. Anti-CD68 and anti-NOS2 antibodies were detected by a A633-goat anti-rabbit IgG and a A488-goat anti-mouse IgG, respectively. Confocal microscopy was performed on a Zeiss LSM700 assembly with 405, 488, 543, and 633nm excitation lines. Data were compiled using ZEN software (Zeiss, Thornton, NY). Quantification of macrophage infiltration was performed in confocal images of infiltrated tissues captured at a magnification of ×600. The cell counts for each condition was obtained by combing data from three mice with three to six sections each.

All cell counting and image processing were performed with ImageJ software. Total DAPI/cell counts in each ROI was automatically obtained using a customized Macro (see Supplementary Materials). For each macrophage marker, the mean count per unit area (~0.028 mm^2, the entire area of an image at ×600 magnification) was obtained in 10–15 ROIs per tissue section, 3 tissue sections per mouse (n=4 for sham group, n=6 for anterior puncture group). For human surgical discarded tissues, the dense AF region was excluded from the analysis based on its high autofluorescence and fibrous structure.

Statistical analysis

Statistical analysis was performed using Prism software (GraphPad Software, La Jolla, CA). Statistical analysis of immunohistochemistry results among three groups at each time point was assessed by one-way ANOVA followed by a Tukey multiple comparison test. Analysis of immunofluorescence results between two groups was performed using t-test. For behavior assay, statistical significance was determined using 2-way ANOVA followed by Bonferroni's multiple comparisons test. A p value <0.05 was considered statistically significant. Data are presented as mean ± standard error of mean (SEM).

Results

Lateral disc puncture with spinal nerve exposure induced mechanical hyperalgesia

Mechanical hyperalgesia was assessed in both hind paws of mice for up to 16 days after surgery. For ipsilateral (left) sides, significant and sustained declines in mechanical threshold were detected in the lateral puncture with nerve exposure group from POD 6 ($*p<0.05$ *vs* nerve exposure group, $^{\#}p<0.05$ *vs* anterior puncture group). Neither nerve exposure nor anterior puncture group exhibited changes in paw withdrawal threshold at the same time period compared to their respective baseline levels (Fig. 2a). For contralateral (right) sides, the three groups demonstrated no statistical difference (Fig. 2b). Transient reductions of mechanical thresholds at early time points, such as POD 2 and POD 4, might be attributed to acute response after surgeries (Fig. 2a, 2b).

Histology and MRI confirmed needle puncture induced disc herniation

The discs of nerve exposure group exhibited normal structure and cellularity with abundant proteoglycan in the NP region, well-organized and concentrically aligned collagen lamellae in the AF region, and a clear boundary between NP and AF (Fig. 3 top row). As expected, on POD 7, discs in both anterior puncture and lateral puncture + nerve exposure groups demonstrated typical signs of disc degeneration, such as diminished NP cellularity, destroyed AF/NP boundary, enlarged chondrocytes, ruptured AF lamina (black arrows, needle puncture sites) and herniated NP tissue (chondrocyte-like cells, red arrows) surrounded by massively cellular infiltration (Fig. 3). Histology of disc puncture groups showed a similar degenerative trend with some cell infiltration observed at hernia sites on POD 3 (red arrows, Supplementary Figure 2).

Degenerative change in discs was also confirmed by MRI. Mid-sagittal T2 weighted MRI demonstrated a decrease in disc signal intensity at 16 days after disc puncture surgery (red arrowheads) in both anterior puncture and the lateral puncture with nerve exposure

groups while the nerve exposure group showed that signal was retained (white arrowhead) (Supplementary Figure 3)

Disc herniation elicited abundant macrophages infiltration and elevation of pro-inflammatory cytokines

Iba-1, a microglia/macrophage-specific marker, was used to assess the infiltration of macrophages on POD 3 and POD 7. By immunohistochemistry, on POD 7, we detected very few Iba-1$^+$ macrophages in the nerve exposure group (upper row, Fig 4a) and abundant macrophages in both punctured groups (middle and lower rows, Fig 4a) at the disc hernia sites (black arrows). In the lateral puncture + nerve exposure group, Iba-1$^+$ brown signals were also detected abundantly surrounding the spinal nerves (Fig. 4). On POD 3, Iba-1$^+$ cells in all three groups appeared less than in POD 7 (Supplementary Figure 4).

As macrophages exert their function through inflammatory mediators, we also analyzed cytokine expression in this newly developed murine radiculopathy model. Production of IL-1β and IL-6 elevated at disc hernia sites of both disc punctured groups (Fig. 4, Supplementary Figure 4), compared to the nerve exposure group at both time points. The elevated cytokine expression was also observed in the area surrounding nerves of lateral puncture with nerve exposure group but not in the traditional anterior puncture group. Quantification of positive signals is shown in Fig. 4b–d, Supplementary Figure 4b–d).

Mixed phenotypes of macrophages infiltrate at hernia sites

Due to the abundance of infiltrated macrophages at hernia sites as we described in our prior research [24] and in the current study, phenotypic characterization of these infiltrated macrophages is particularly important to understand the roles of macrophages in disease progression. Since the anterior puncture elicited similar abundant macrophage infiltration at disc hernia sites to the lateral puncture + nerve exposure group, anterior puncture model was employed to study sub-phenotypes of infiltrated macrophages on POD 7 by immunostaining. Significantly more total infiltrating cells (DAPI counts) were consistently detected in disc puncture group compared to the sham group (**p<0.01, > 4 folds, Fig. 5a–5b). Additionally, CD68$^+$, F4/80$^+$, and CD11b$^+$ macrophages were abundantly detected in the inflammatory tissue of the punctured group compared to shams (by ~8–40 folds, Fig. 5). Both iNOS$^+$ (M1 marker, ~7 folds) and MMR$^+$ (M2 marker, ~23 folds) macrophages were detected in the puncture group with a few iNOS$^+$MMR$^+$ cells found in some regions (white arrow, Fig. 6a). Quantitative analysis showed ~10% iNOS$^+$ and ~30% MMR$^+$ macrophages in the puncture group (Fig. 6d, 6e). IgG control exhibited no comparable signals (Supplementary Figure 5*)*.

As shown in Fig. 7, we also detected abundant macrophages (75 ± 3.4%) in inflammatory disc tissues from 4 patients that had undergone discectomy surgery while AF regions were excluded from this (Supplementary Figure 6*)*. The majority of these cells were CD68$^+$ (pan marker) and CD163$^+$ (M2 marker) with small populations of macrophages were CD80$^+$ (M1 marker) and CD80$^+$CD163$^+$ (M1/M2, white arrow, Fig. 7).

Increased Iba1+ macrophages but unaltered GFAP+ astrocytes in injured nerves

Immunohistochemistry on POD 7 showed markedly increased Iba1$^+$ signal in the ipsilateral nerve of lateral puncture + nerve exposure group (Fig. 8). However, expression of GFAP, an astrocyte and glial cell marker, showed no differences (Supplementary Figure 8).

Discussion

Since 1934, compression of the nerve root by disc herniation has been considered to be the cause of sciatica. Although a surgical procedure, such as laminectomy, has become the gold standard to alleviate pain, it may not be effective in some cases. Moreover, nerve compression has been observed in patients with asymptomatic disc herniation also. By contrast, in some patients with severe sciatica, nerve compression was not detected, therefore, the level of pain may often be disproportionate to the severity of disc herniation [35–37], which is a paradox in the field.

A mouse model is suitable for the study of disc herniation because it can be manipulated genetically in ways that represent human conditions [38], which a large animal models do not offer. To better understand the problem of disc herniation, a clinically relevant animal model is highly desirable since neither the existing anterior annulus puncture model nor the posterior model can reproduce the clinical scenario in humans. The widely used anterior annulus puncture model does not induce radiculopathy since the herniated disc tissue (anterior) is located anatomically distant from the nerve root or epidural space (posterior) and incapable of eliciting pain sensation [39]. In previously reported posterior annulus puncture models [40,41], one side of the facet joint was typically removed to expose the discs, which led to confounding attribution of pain. Specifically, radiculopathy and pain induced in the posterior puncture models can be caused by both biomechanical spine instability (due to facet joint damage) and biochemical responses (due to disc herniation), however, these two conditions rarely co-exist in the patient at the same time. By contrast, the NP autograft transplantation model was developed to simulate nerve compression-induced radiculopathy by implanting tail disc NP material proximal to the lumbar nerve roots [26,42]. Although this model might provide information regarding the nerve sensitization and potential molecular targets to address radicular pain, laminectomy is required to uncover the nerves, which also induces pain and is commonly complicated with iatrogenic neural injury. Additionally, in this NP implantation model, the lumbar discs remain intact, which is different from human disc herniation.

Considering the advantages and disadvantages of these animal models, we have developed a new radiculopathy mouse model involving both lateral disc puncture and spinal nerve exposure to enable direct interaction of herniated NP tissues with nearby nerves. As shown in Fig. 2, this new model induced sustained radiculopathy on the ipsilateral side compared to control groups, which supported our model design hypothesis. The transient decline in the mechanical threshold on POD 2 and POD4 might attribute to surgical procedure or nerve irritation. Elevated pain levels in the experimental group are corroborated by abundant infiltration of Iba1$^+$ macrophages and expression of IL-1β and IL-6 detected at disc hernia sites and near exposed nerves (Fig. 4), which might collectively contribute to pain sensitivity. For the traditional anterior disc puncture group, despite a significant

increase in macrophage infiltration and proinflammatory cytokines production, ipsilateral mechanical threshold exhibited negligible changes compared to the baseline and nerve exposure group (Fig. 2) since herniation-induced inflammatory responses were spatially distant from nerves (Fig. 3, Fig. 4). Therefore, within the experimental setting of this study, our new animal model (lateral disc puncture with nerve exposure) could replicate the clinical symptoms of herniation induced radicular pain in humans. Moreover, this model can also be reproduced in most laboratories that are equipped with animal surgery.

Discogenic radiculopathy involves a complex array of biochemical and biomechanical factors, such as local inflammatory responses and nerve compression due to NP protrusion. Over the past two decades, research suggested that inflammatory responses, involving immune cell infiltration and various mediators, play a critical role in disc herniation induced pain. Literature reported upregulation of a variety of immune mediators in disc herniation, including pro-inflammatory cytokines (IL-1, TNF-α, IL-6), anti-inflammatory cytokines (TGF-β, IL-4, IL-10), and chemokines (MCP-1, MIP-1, IP-10) [43–45]. In addition, abundant macrophages have been detected in inflammatory disc tissues at hernia sites in both mice and humans. For example, our previously reported study using immunohistochemistry, in a mouse model of disc herniation, showed that neutrophils appeared on POD 1, remained visible on POD 3, but were not detectable on POD 7, while few macrophages were present on POD 1, significantly increased on POD 3, and infiltrated abundantly on POD 7 [24]. In autologous NP transplantation animal models, abundant macrophages and some leukocytes (T cells, B cells, and NK cells) were identified at transplanted disc sites [7,8]. Lymphocytes (T/B cells) were also detected in human herniated disc tissues [46,47]. In the newly established model, our results confirmed massive macrophage infiltration (Iba-1^+ cells) and abundantly elevated proinflammatory cytokines IL-1β and IL-6, surrounding the herniated NP near the exposed nerve (Fig. 4). This data suggests that macrophages might be important immune players in the inflammatory and resorption processes of herniated discs.

Prior studies typically adopted immunohistochemistry to detect macrophages in murine and human samples. To avoid outcome variation due to long sample fixation and processing, we adopted a mild fixation procedure whereby antigen especially cell surface markers (CD11b, F4/80, MMR, etc.) can be well-preserved [48] and direct immunostaining to analyze dissected inflammatory tissues. Using this method, we detected a significant increase of $CD68^+$ macrophages as well as $CD11b^+$ and $F4/80^+$ macrophages in the infiltrated tissue of punctured discs compared to sham discs (Fig. 5). Although the traditional macrophage classification (M1 vs M2) is a well-known and valuable concept, emerging evidence suggests that macrophage phenotypes may be more appropriately described as a continuum of functional states that are plastic and signal-dependent [49,50]. For example, MMR and iNOS were used for decades to assign M2- and M1-phenotypes, respectively. However, these markers were recently found to be co-expressed within the same cell clusters [51–54]. Indeed, we detected a large number of MMR^+ macrophages (~30%) and a small fraction of $iNOS^+$ macrophages (~10%) in the acute phase of disc herniation on POD 7 and a small cluster of $iNOS^+MMR^+$ population using immunofluorescence staining (Fig. 6, Fig. 7). Such heterogeneous nature of macrophages was also detected in human samples of acute disc herniation, surgically dissected from patients with a 3–6 months' duration

from disease onset to discectomy. Our findings aligned with the study by Nakawaki et al showing elevated mRNA expression of M1 and M2 macrophage markers from POD 1 [55], suggesting that heterogeneous macrophage populations, including myeloid lineage and resident macrophages, as well as different sub-phenotypes, are involved in the pathology of disc herniation.

In addition to the impact of environmental cues at the disc hernia site, inflammatory responses in DRGs and nerve roots is also critical to the pathology of radiculopathy. For example, literature reported autograft model suggested that the disc itself served as an inflammatory material causing mechanical hyperalgesia and neuropathic pain [56]. Intra-discal injection of Complete Freund's Adjuvant (water in oil emulsion contains inactivated mycobacteria) led to disc degeneration in rats with increased expression of pro-inflammatory prostaglandin E2, iNOS, and neuropeptide calcitonin gene-related peptide in both discs and DRGs that was responsible for allodynia and pain behavior [57]. Ohtori *et al.* also reported that epidural injection of TNF-α inhibitor etanercept (a TNF Receptor-IgG fusion protein) or IL-6 blocker tocilizumab (an anti-IL-6R monoclonal antibody) relieved radicular pain associated with lumbar stenosis [58]. In our study, markedly increased $Iba1^{+}$ macrophages/microglial were also detected in the ipsilateral nerve of lateral puncture with nerve exposure group (Fig. 8), suggesting the infiltration and activation of macrophages/microglia in nerves in the context of disc herniation induced radiculopathy. Despite the observation that the astrocyte and glial cell marker, GFAP did not show any differences among the groups (Supplementary Figure 8), the roles of astrocytes in pain transmission cannot be ruled out because astrogliosis may occur at different timeframes [59], and this warrants further investigation.

There are several limitations in the current study. First, the observation window is relatively short, an extended investigation (up to months) might help assess outcomes of long-term pathology. Second, this model stimulates radiculopathy caused by far-lateral disc herniation, which is located lateral to the foramen. A posterior approach with laminectomy and dura retraction needs to be adopted to access the small-sized lateral recess with microsurgical instruments, which would be challenging technically for those not equipped with microsurgery techniques. Third, further analysis on spinal nerves and DRGs is necessary to better elucidate the molecular crosstalk between the herniated disc and nerves. Future studies may include mechanisms of neuron excitation and neuropeptide release, comparison of this model with the NP autograft or local cytokine injection models would help elucidate the strengths of these experimental approaches. In addition, characterizing macrophage phenotypes at various disease stages of disc herniation is highly desirable and will be our focus for future investigation.

In summary, we established a new mouse model to mimic the human condition of acute radiculopathy, which induced significant and sustained ipsilateral pain and abundant macrophage infiltration and proinflammatory cytokine production in the niche of disc herniation. Our model may serve as a tool to investigate interactions among disc herniation, the immune system and neuropathic pain, and enable screening of novel therapies.

Supplementary Material

Refer to Web version on PubMed Central for supplementary material.

Funding Disclosure Statement:

We are grateful for financial support from the National Institutes of Health (NIAMS AR072334, AR064792, and AR078547) and the Commonwealth Health Research Board. The research was conducted in the absence of any commercial or financial relationships that could be construed as a potential conflict of interest.

Abbreviation

IVD	intervertebral disc
NP	nucleus pulposus
AF	annulus fibrosus
DRG	dorsal root ganglion
POD	post-operative day
IL-1	interleukin-1
IL-6	interleukin-6
IL-4	interleukin-4
IL-10	interleukin-10 GFAP, glial fibrillary acidic protein
Iba-1	ionized calcium binding adaptor molecule 1
MMR	macrophage mannose receptor
NK	natural killer cells
TNF-α	tumor necrosis factor – alpha
iNOS	inducible nitric oxide synthase
TGF-β	transforming growth factor – beta
MCP-1	monocyte chemoattractant protein-1
MIP-1	macrophage inflammatory protein
DAPI, 4′	6-diamidino-2-phenylindole
GFP	green fluorescence protein

References

[1]. Deyo RA, Tsui-Wu YJ. Descriptive epidemiology of low-back pain and its related medical care in the United States. Spine 1987;12:264–268. doi:10.1097/00007632-198704000-00013. [PubMed: 2954221]

[2]. Martin BI, Deyo RA, Mirza SK, Turner JA, Comstock BA, Hollingworth W, et al. Expenditures and health status among adults with back and neck problems. JAMA 2008;299:656–664. doi:10.1001/jama.299.6.656. [PubMed: 18270354]

[3]. Andersson GB. Epidemiological features of chronic low-back pain. Lancet 1999;354:581–585. doi:10.1016/S0140-6736(99)01312-4. [PubMed: 10470716]

[4]. Gray DT, Deyo RA, Kreuter W, Mirza SK, Heagerty PJ, Comstock BA, et al. Population-based trends in volumes and rates of ambulatory lumbar spine surgery. Spine 2006;31:1957–63; discussion 1964. doi:10.1097/01.brs.0000229148.63418.c1. [PubMed: 16924213]

[5]. Geurts JW, Willems PC, Kallewaard J-W, van Kleef M, Dirksen C. The impact of chronic discogenic low back pain: costs and patients' burden. Pain Res Manag 2018;2018:4696180. doi:10.1155/2018/4696180. [PubMed: 30364097]

[6]. van der Windt DA, Simons E, Riphagen II, Ammendolia C, Verhagen AP, Laslett M, et al. Physical examination for lumbar radiculopathy due to disc herniation in patients with low-back pain. Cochrane Database Syst Rev 2010:CD007431. doi:10.1002/14651858.CD007431.pub2. [PubMed: 20166095]

[7]. Murai K, Sakai D, Nakamura Y, Nakai T, Igarashi T, Seo N, et al. Primary immune system responders to nucleus pulposus cells: evidence for immune response in disc herniation. Eur Cell Mater 2010;19:13–21. doi:10.22203/ecm.v019a02. [PubMed: 20077401]

[8]. Geiss A, Sobottke R, Delank KS, Eysel P. Plasmacytoid dendritic cells and memory T cells infiltrate true sequestrations stronger than subligamentous sequestrations: evidence from flow cytometric analysis of disc infiltrates. Eur Spine J 2016;25:1417–1427. doi:10.1007/s00586-015-4325-z. [PubMed: 26906170]

[9]. Kawaguchi S, Yamashita T, Katahira G, Yokozawa H, Torigoe T, Sato N. Chemokine profile of herniated intervertebral discs infiltrated with monocytes and macrophages. Spine 2002;27:1511–1516. [PubMed: 12131709]

[10]. Kawaguchi S, Yamashita T, Yokogushi K, Murakami T, Ohwada O, Sato N. Immunophenotypic analysis of the inflammatory infiltrates in herniated intervertebral discs. Spine 2001;26:1209–1214. doi:10.1097/00007632-200106010-00008. [PubMed: 11389385]

[11]. Willems N, Tellegen AR, Bergknut N, Creemers LB, Wolfswinkel J, Freudigmann C, et al. Inflammatory profiles in canine intervertebral disc degeneration. BMC Vet Res 2016;12:10. doi:10.1186/s12917-016-0635-6. [PubMed: 26757881]

[12]. Mills CD, Lenz LL, Ley K. Macrophages at the fork in the road to health or disease. Front Immunol 2015;6:59. doi:10.3389/fimmu.2015.00059. [PubMed: 25762997]

[13]. Mills CD, Harris RA, Ley K. Macrophage Polarization: Decisions That Affect Health. J Clin Cell Immunol 2015;6. doi:10.4172/2155-9899.1000364.

[14]. Shapouri-Moghaddam A, Mohammadian S, Vazini H, Taghadosi M, Esmaeili S-A, Mardani F, et al. Macrophage plasticity, polarization, and function in health and disease. J Cell Physiol 2018;233:6425–6440. doi:10.1002/jcp.26429.

[15]. Martinez FO, Gordon S. The M1 and M2 paradigm of macrophage activation: time for reassessment. F1000Prime Rep 2014;6:13. doi:10.12703/P6-13. [PubMed: 24669294]

[16]. Baba H, Maezawa Y, Furusawa N, Fukuda M, Uchida K, Kokubo Y, et al. Herniated cervical intervertebral discs: histological and immunohistochemical characteristics. Eur J Histochem 1997;41:261–270. [PubMed: 9491312]

[17]. Kokubo Y, Uchida K, Kobayashi S, Yayama T, Sato R, Nakajima H, et al. Herniated and spondylotic intervertebral discs of the human cervical spine: histological and immunohistological findings in 500 en bloc surgical samples. Laboratory investigation. J Neurosurg Spine 2008;9:285–295. doi:10.3171/SPI/2008/9/9/285. [PubMed: 18928227]

[18]. Koike Y, Uzuki M, Kokubun S, Sawai T. Angiogenesis and inflammatory cell infiltration in lumbar disc herniation. Spine 2003;28:1928–1933. doi:10.1097/01.BRS.0000083324.65405.AE. [PubMed: 12973136]

[19]. Arai Y, Yasuma T, Shitoto K, Yamauchi Y, Suzuki F. Immunohistological study of intervertebral disc herniation of lumbar spine. J Orthop Sci 2000;5:229–231. doi:10.1007/s007760050156. [PubMed: 10982662]

[20]. Kawakubo A, Uchida K, Miyagi M, Nakawaki M, Satoh M, Sekiguchi H, et al. Investigation of resident and recruited macrophages following disc injury in mice. J Orthop Res 2020;38:1703–1709. doi:10.1002/jor.24590. [PubMed: 31965590]

[21]. Vizcaíno Revés N, Mogel HM, Stoffel M, Summerfield A, Forterre F. Polarization of macrophages in epidural inflammation induced by canine intervertebral disc herniation. Front Vet Sci 2020;7:32. doi:10.3389/fvets.2020.00032. [PubMed: 32083108]

[22]. Gertzbein SD. Degenerative disk disease of the lumbar spine: immunological implications. Clin Orthop Relat Res 1977:68–71. doi:10.1097/00003086-197711000-00007.

[23]. Gertzbein SD, Tait JH, Devlin SR. The stimulation of lymphocytes by nucleus pulposus in patients with degenerative disk disease of the lumbar spine. Clin Orthop Relat Res 1977:149–154.

[24]. Xiao L, Ding M, Zhang Y, Chordia M, Pan D, Shimer A, et al. A novel modality for functional imaging in acute intervertebral disk herniation via tracking leukocyte infiltration. Mol Imaging Biol 2017;19:703–713. doi:10.1007/s11307-016-1038-6. [PubMed: 28050750]

[25]. Liang H, Ma S-Y, Feng G, Shen FH, Joshua Li X. Therapeutic effects of adenovirus-mediated growth and differentiation factor-5 in a mice disc degeneration model induced by annulus needle puncture. Spine J 2010;10:32–41. doi:10.1016/j.spinee.2009.10.006. [PubMed: 19926342]

[26]. Jin L, Ding M, Oklopcic A, Aghdasi B, Xiao L, Li Z, et al. Nanoparticle fullerol alleviates radiculopathy via NLRP3 inflammasome and neuropeptides. Nanomedicine 2017;13:2049–2059. doi:10.1016/j.nano.2017.03.015. [PubMed: 28404518]

[27]. Xiao L, Ding M, Fernandez A, Zhao P, Jin L, Li X. Curcumin alleviates lumbar radiculopathy by reducing neuroinflammation, oxidative stress and nociceptive factors. Eur Cell Mater 2017;33:279–293. doi:10.22203/eCM.v033a21. [PubMed: 28485773]

[28]. Xiao L, Hong K, Roberson C, Ding M, Fernandez A, Shen F, et al. Hydroxylated Fullerene: A Stellar Nanomedicine to Treat Lumbar Radiculopathy via Antagonizing TNF-α-Induced Ion Channel Activation, Calcium Signaling, and Neuropeptide Production. ACS Biomater Sci Eng 2018;4:266–277. doi:10.1021/acsbiomaterials.7b00735. [PubMed: 30038959]

[29]. Zhang D, Jin L, Reames DL, Shen FH, Shimer AL, Li X. Intervertebral disc degeneration and ectopic bone formation in apolipoprotein E knockout mice. J Orthop Res 2013;31:210–217. doi:10.1002/jor.22216. [PubMed: 22915292]

[30]. Jin L, Liu Q, Scott P, Zhang D, Shen F, Balian G, et al. Annulus fibrosus cell characteristics are a potential source of intervertebral disc pathogenesis. PLoS One 2014;9:e96519. doi:10.1371/journal.pone.0096519. [PubMed: 24796761]

[31]. Xiao L, Majumdar R, Dai J, Li Y, Xie L, Shen FH, et al. Molecular detection and assessment of intervertebral disc degeneration via a collagen hybridizing peptide. ACS Biomater Sci Eng 2019;5:1661–1667. doi:10.1021/acsbiomaterials.9b00070. [PubMed: 31788555]

[32]. Mclean IW, Nakane PK. PERIODATE-LYSINE-PARAFORMALDEHYDE FIXATIVE A NEW FIXATIVE FOR IMMUNOELECTRON MICROSCOPY. Journal of Histochemistry & Cytochemistry 1974;22:1077–1083. doi:10.1177/22.12.1077. [PubMed: 4374474]

[33]. Sung SJ, Fu SM. - Interactions among glomerulus infiltrating macrophages and intrinsic cells via. - J Autoimmun 2020 Jan;106:102331 doi: 101016/j.jaut2019102331 Epub 2019 Sep 5 n.d.:-102331. [PubMed: 31495649]

[34]. Sung S-SJ, Ge Y, Dai C, Wang H, Fu SM, Sharma R, et al. Dependence of Glomerulonephritis Induction on Novel Intraglomerular Alternatively Activated Bone Marrow-Derived Macrophages and Mac-1 and PD-L1 in Lupus-Prone NZM2328 Mice. J Immunol 2017;198:2589–2601. doi:10.4049/jimmunol.1601565. [PubMed: 28219886]

[35]. Lorio M, Kim C, Araghi A, Inzana J, Yue JJ. International Society for the Advancement of Spine Surgery Policy 2019-Surgical Treatment of Lumbar Disc Herniation with Radiculopathy. Int J Spine Surg 2020;14:1–17. doi:10.14444/7001. [PubMed: 32128297]

[36]. Rogerson A, Aidlen J, Jenis LG. Persistent radiculopathy after surgical treatment for lumbar disc herniation: causes and treatment options. Int Orthop 2019;43:969–973. doi:10.1007/s00264-018-4246-7. [PubMed: 30498910]

[37]. Djuric N, Yang X, Ostelo RWJG, van Duinen SG, Lycklama À Nijeholt GJ, van der Kallen BFW, et al. Disc inflammation and Modic changes show an interaction effect on recovery after surgery

for lumbar disc herniation. Eur Spine J 2019;28:2579–2587. doi:10.1007/s00586-019-06108-9. [PubMed: 31440895]

[38]. Showalter BL, Beckstein JC, Martin JT, Beattie EE, Espinoza Orías AA, Schaer TP, et al. Comparison of animal discs used in disc research to human lumbar disc: torsion mechanics and collagen content. Spine 2012;37:E900–7. doi:10.1097/BRS.0b013e31824d911c. [PubMed: 22333953]

[39]. Jin L, Balian G, Li XJ. Animal models for disc degeneration-an update. Histol Histopathol 2018;33:543–554. doi:10.14670/HH-11-910. [PubMed: 28580566]

[40]. Li Z, Liu H, Yang H, Wang J, Wang H, Zhang K, et al. Both expression of cytokines and posterior annulus fibrosus rupture are essential for pain behavior changes induced by degenerative intervertebral disc: An experimental study in rats. J Orthop Res 2014;32:262–272. doi:10.1002/jor.22494. [PubMed: 24115280]

[41]. Olmarker K Puncture of a lumbar intervertebral disc induces changes in spontaneous pain behavior: an experimental study in rats. Spine 2008;33:850–855. doi:10.1097/BRS.0b013e31816b46ca. [PubMed: 18404103]

[42]. de Souza Grava AL, Ferrari LF, Defino HLA. Cytokine inhibition and time-related influence of inflammatory stimuli on the hyperalgesia induced by the nucleus pulposus. Eur Spine J 2012;21:537–545. doi:10.1007/s00586-011-2027-8. [PubMed: 21947908]

[43]. Cunha C, Silva AJ, Pereira P, Vaz R, Gonçalves RM, Barbosa MA. The inflammatory response in the regression of lumbar disc herniation. Arthritis Res Ther 2018;20:251. doi:10.1186/s13075-018-1743-4. [PubMed: 30400975]

[44]. Risbud MV, Shapiro IM. Role of cytokines in intervertebral disc degeneration: pain and disc content. Nat Rev Rheumatol 2014;10:44–56. doi:10.1038/nrrheum.2013.160. [PubMed: 24166242]

[45]. Djuric N, Lafeber GCM, Vleggeert-Lankamp CLA. The contradictory effect of macrophage-related cytokine expression in lumbar disc herniations: a systematic review. Eur Spine J 2020;29:1649–1659. doi:10.1007/s00586-019-06220-w. [PubMed: 31768840]

[46]. Geiss A, Larsson K, Junevik K, Rydevik B, Olmarker K. Autologous nucleus pulposus primes T cells to develop into interleukin-4-producing effector cells: an experimental study on the autoimmune properties of nucleus pulposus. J Orthop Res 2009;27:97–103. doi:10.1002/jor.20691. [PubMed: 18634006]

[47]. Park JB, Chang H, Kim KW. Expression of Fas ligand and apoptosis of disc cells in herniated lumbar disc tissue. Spine 2001;26:618–621. [PubMed: 11246372]

[48]. Sung S-SJ. Co-immunostaining of ICAM-1, ICAM-2, and CD31 in Mouse Kidney Glomeruli. Bio Protoc 2020;10:e3663. doi:10.21769/BioProtoc.3663.

[49]. Buscher K, Ehinger E, Gupta P, Pramod AB, Wolf D, Tweet G, et al. Natural variation of macrophage activation as disease-relevant phenotype predictive of inflammation and cancer survival. Nat Commun 2017;8:16041. doi:10.1038/ncomms16041. [PubMed: 28737175]

[50]. Orecchioni M, Ghosheh Y, Pramod AB, Ley K. Macrophage Polarization: Different Gene Signatures in M1(LPS+) vs. Classically and M2(LPS−) vs. Alternatively Activated Macrophages. Front Immunol 2019;10:1084. doi:10.3389/fimmu.2019.01084. [PubMed: 31178859]

[51]. Maloney J, Keselman A, Li E, Singer SM. Macrophages expressing arginase 1 and nitric oxide synthase 2 accumulate in the small intestine during Giardia lamblia infection. Microbes Infect 2015;17:462–467. doi:10.1016/j.micinf.2015.03.006. [PubMed: 25797399]

[52]. Schleicher U, Paduch K, Debus A, Obermeyer S, König T, Kling JC, et al. TNF-Mediated Restriction of Arginase 1 Expression in Myeloid Cells Triggers Type 2 NO Synthase Activity at the Site of Infection. Cell Rep 2016;15:1062–1075. doi:10.1016/j.celrep.2016.04.001. [PubMed: 27117406]

[53]. Redente EF, Higgins DM, Dwyer-Nield LD, Orme IM, Gonzalez-Juarrero M, Malkinson AM. Differential polarization of alveolar macrophages and bone marrow-derived monocytes following chemically and pathogen-induced chronic lung inflammation. J Leukoc Biol 2010;88:159–168. doi:10.1189/jlb.0609378. [PubMed: 20360403]

[54]. Kraus VB, McDaniel G, Huebner JL, Stabler TV, Pieper CF, Shipes SW, et al. Direct in vivo evidence of activated macrophages in human osteoarthritis. Osteoarthr Cartil 2016;24:1613–1621. doi:10.1016/j.joca.2016.04.010.

[55]. Nakawaki M, Uchida K, Miyagi M, Inoue G, Kawakubo A, Kuroda A, et al. Sequential CCL2 expression profile after disc injury in mice. J Orthop Res 2019. doi:10.1002/jor.24522.

[56]. Takada T, Nishida K, Maeno K, Kakutani K, Yurube T, Doita M, et al. Intervertebral disc and macrophage interaction induces mechanical hyperalgesia and cytokine production in a herniated disc model in rats. Arthritis Rheum 2012;64:2601–2610. doi:10.1002/art.34456. [PubMed: 22392593]

[57]. Lee M, Kim B-J, Lim EJ, Back SK, Lee J-H, Yu S-W, et al. Complete Freund's adjuvant-induced intervertebral discitis as an animal model for discogenic low back pain. Anesth Analg 2009;109:1287–1296. doi:10.1213/ane.0b013e3181b31f39. [PubMed: 19762759]

[58]. Ohtori S, Miyagi M, Eguchi Y, Inoue G, Orita S, Ochiai N, et al. Epidural administration of spinal nerves with the tumor necrosis factor-alpha inhibitor, etanercept, compared with dexamethasone for treatment of sciatica in patients with lumbar spinal stenosis: a prospective randomized study. Spine 2012;37:439–444. doi:10.1097/BRS.0b013e318238af83. [PubMed: 22020607]

[59]. Ji R-R, Donnelly CR, Nedergaard M. Astrocytes in chronic pain and itch. Nat Rev Neurosci 2019;20:667–685. doi:10.1038/s41583-019-0218-1. [PubMed: 31537912]

Highlights

- A new mouse model mimicking human radiculopathy
- Inflammation plays important role in disc herniation and pain
- Heterogeneous macrophages contribute to the pathogenesis of disc herniation

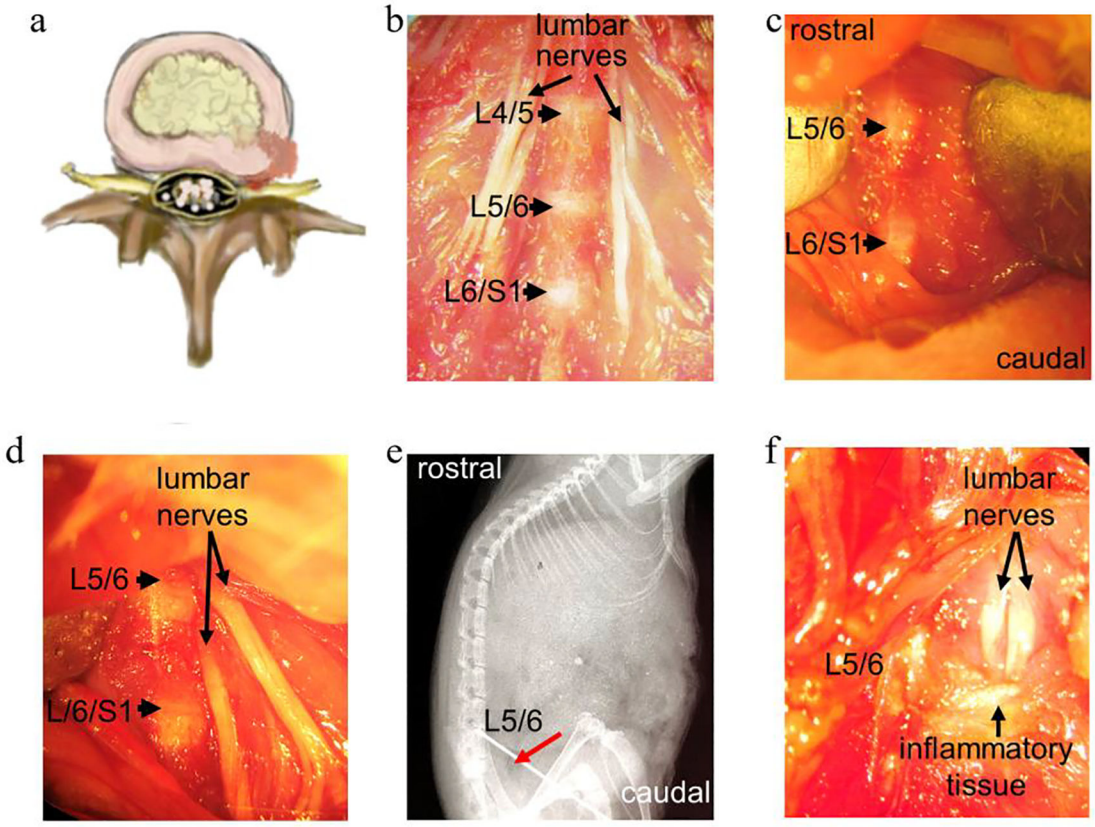

Figure 1. Images demonstrated surgical procedures to establish a mouse model of disc herniation induced radiculopathy (lateral disc puncture with nerve exposure).

(a) A cartoon illustrates the mechanism of disc herniation induced radiculopathy, in which herniated disc tissue protrudes towards the nearby nerves. (b) Macrograph showing the anatomic structure of IVDs and spinal nerves after surgical exposure. (c) Macrograph of exposed L5 and L6 discs prior to needle puncture. (d) Macrograph of exposed discs and adjacent nerves. (e) Sagittal X-ray indicating entry of a needle (red arrow) into the L5/6 disc. (f) Inflammatory tissue surrounding discs and nerves were visualized on POD 7. Images in b-e and f were captured with a Nikon digital camera under a dissecting microscope.

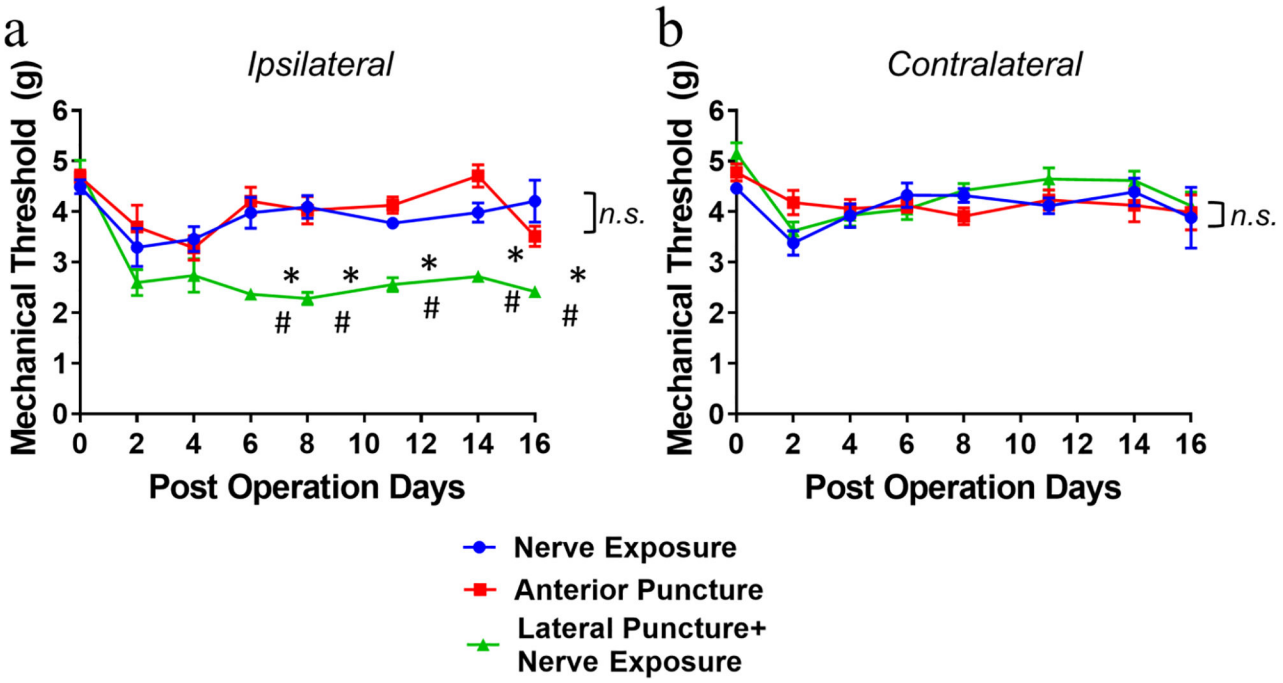

Figure 2. Changes in ipsilateral (a) and contralateral (b) mechanical hyperalgesia of mice for up to 16 days after surgery, measured using an electronic von Frey Aesthesiometer.

Data are presented as mean ± SEM, n=9 per group for the spinal nerve exposure and anterior puncture groups, and n=10 for the lateral puncture with nerve exposure group. Intergroup differences were analyzed by ANOVA with Bonferroni's multiple comparisons test. *p<0.05 indicate differences between lateral puncture with nerve exposure *vs* nerve exposure group, $^{\#}p$<0.05 indicate differences between lateral puncture with nerve exposure *vs* anterior puncture group. *n.s.* indicates no difference in ipsilateral paw withdrawal threshold between nerve exposure and anterior puncture groups in (a) and no difference in contralateral paw withdrawal threshold among three groups in (b).

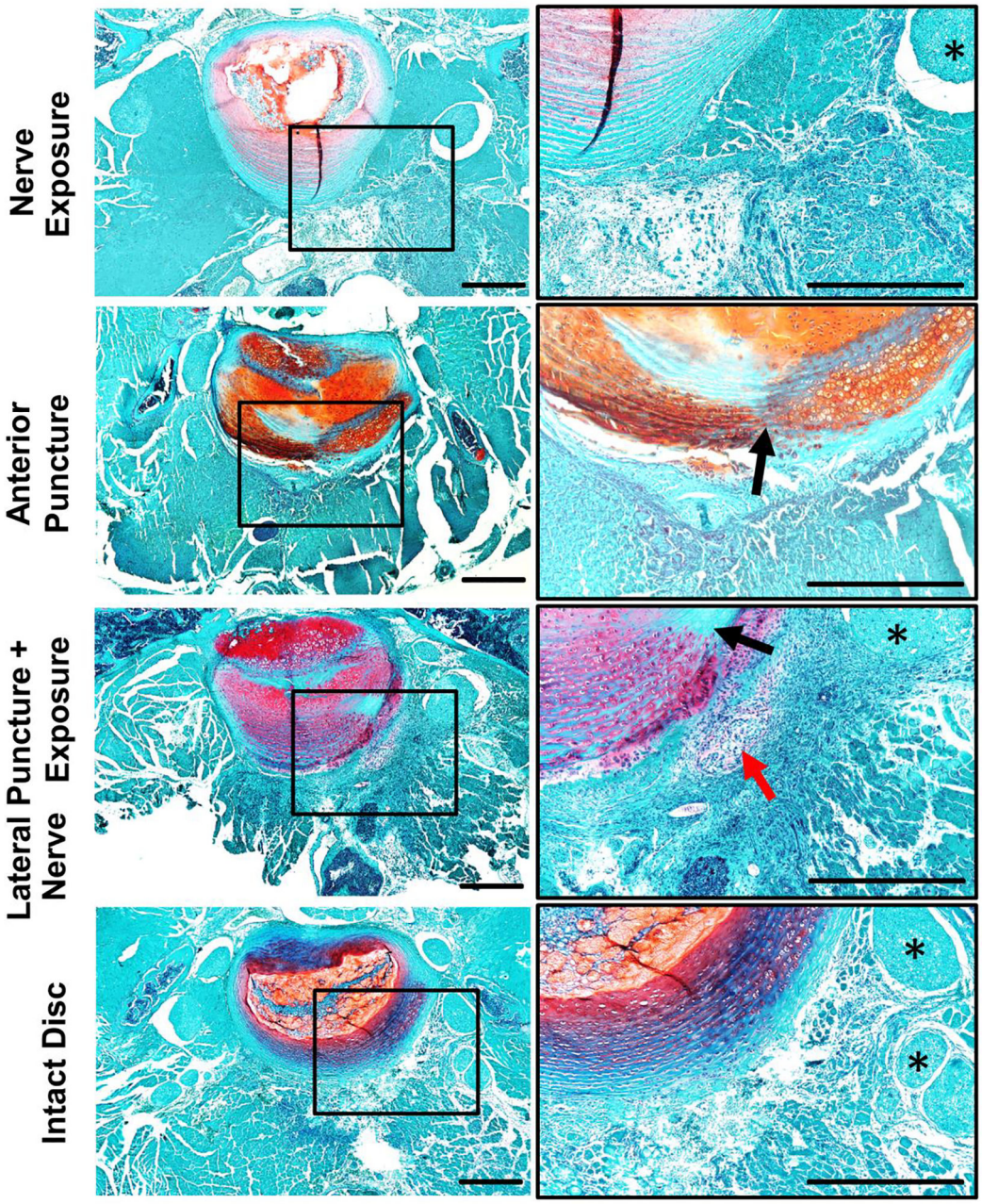

Figure 3. Safranin-O staining shows disrupted structure and abundant cell infiltration in the disc punctured groups on POD 7.

Axial mouse spine sections were stained with Safranin-O. Images were taken at 40× (left) and 200× (right) magnification, respectively. Arrows indicate herniated nucleus pulposus tissue; asterisks indicate nerves. Scale bar=500 μm.

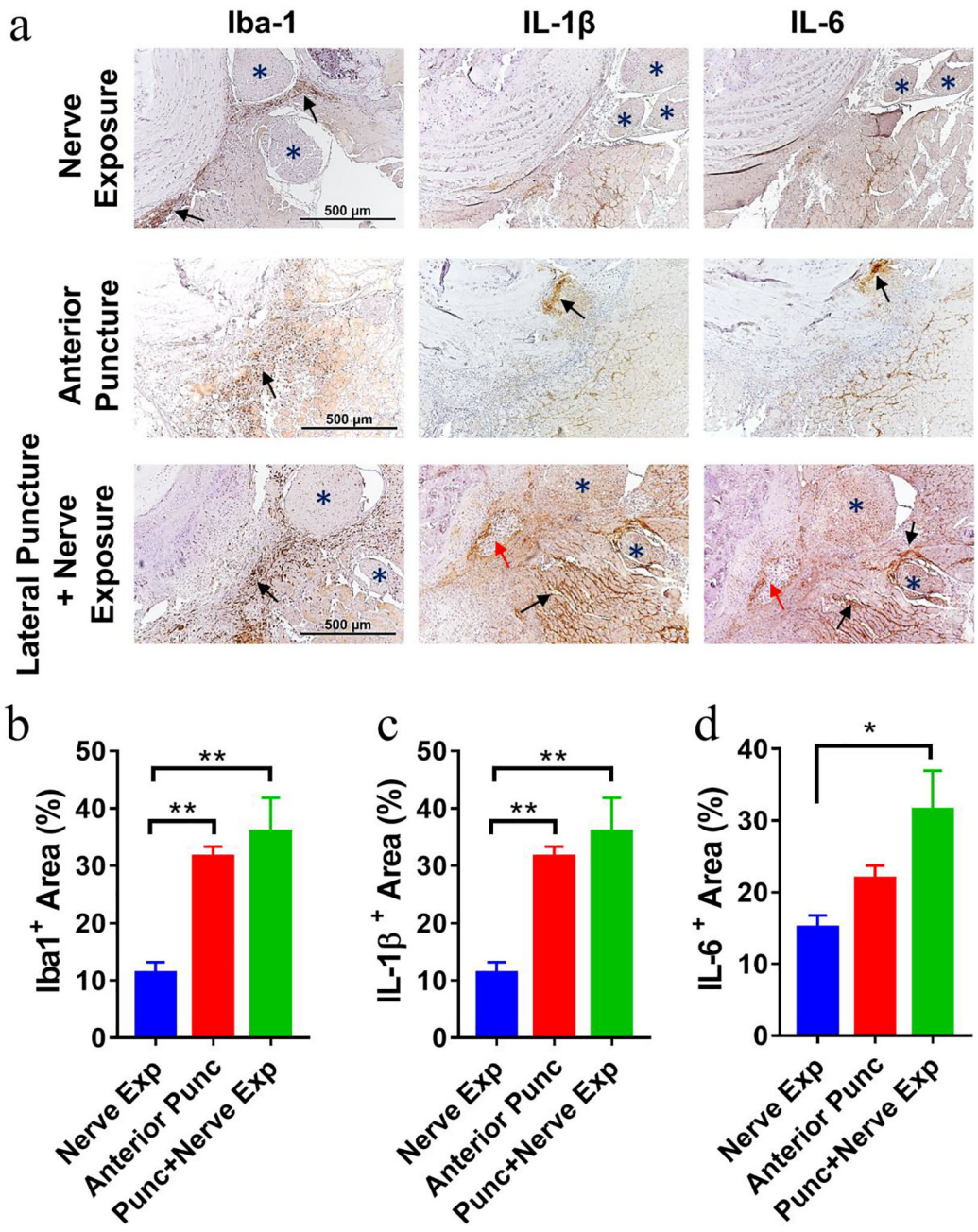

Figure 4. Immunohistochemistry of mouse axial spine sections illustrated massive macrophage infiltration and production of pro-inflammatory cytokines IL-1 and IL-6 in disc punctured groups on POD 7.

(a) Abundant Iba-1^{+} macrophages (left), IL-1β (middle), and IL-6 (right) were detected at disc hernia sites of disc puncture groups, while few Iba-1^{+}, IL-1β, and IL-6 signals were seen in the nerve exposure group. Blue * indicates nerves; Red arrows indicate herniated NP tissue with chondrocyte like morphology; Black arrows indicate positive staining. Images were taken at 200× magnification. Scale bar=500 μm. Quantification of positive immunostaining signal showed Iba1+ macrophages **(b)**, levels of IL-1β **(c)** and IL-6

(d) among three groups. Data are presented as mean ± SEM, n=3–4 per group. *p<0.05, **p<0.01.

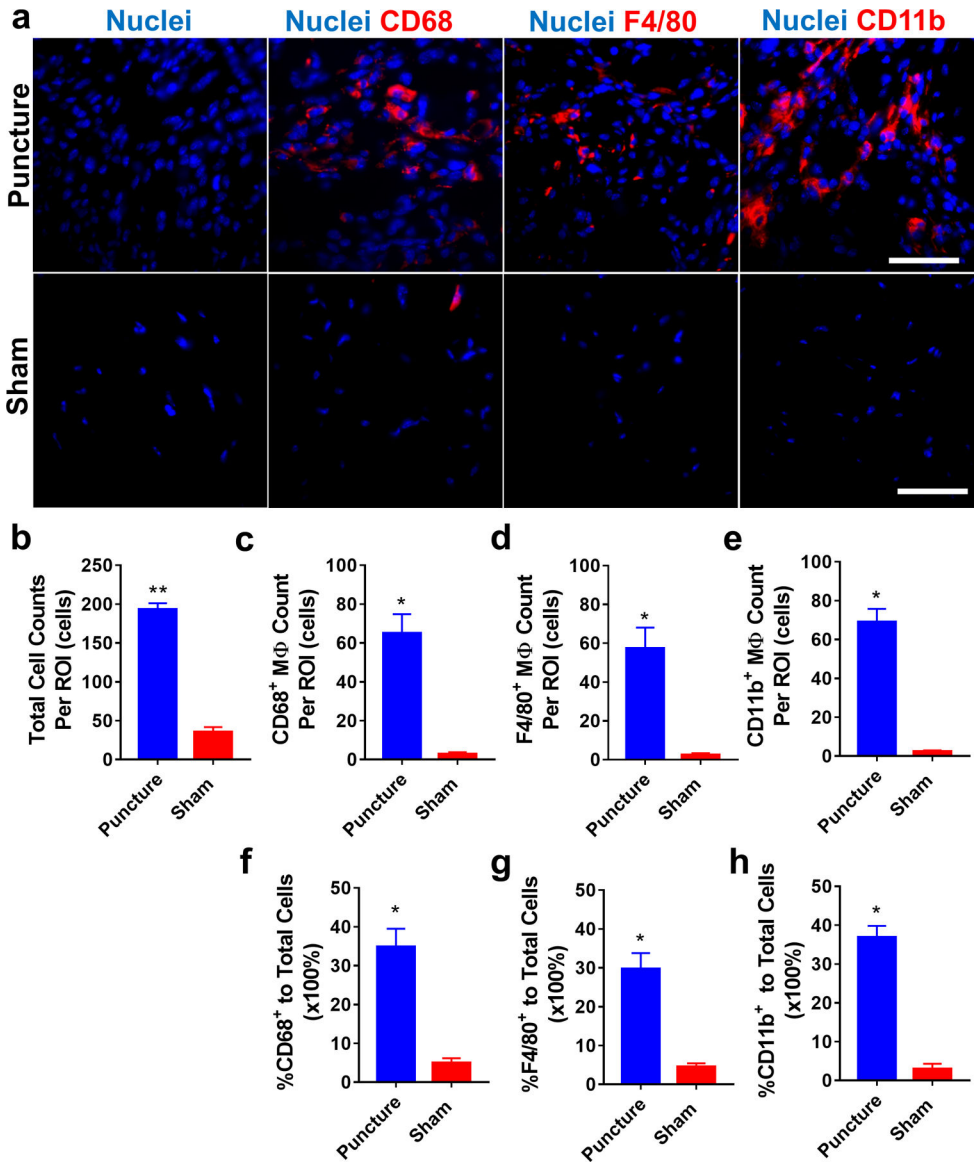

Figure 5. Immunofluorescence staining demonstrated a mixed population of macrophages at disc hernia sites on POD 7 compared to the sham.

(a) Representative fluorescence images showed increased total, $CD68^+$, $F4/80^+$, and $CD11b^+$ macrophages in dissected infiltration tissues of disc punctured mice. The disc puncture group showed significantly more total cells **(b),** $CD68^+$ **(c),** $F4/80^+$ **(d),** and $CD11b^+$ **(e)** macrophages and a greater percentage of macrophage to total cells **(f, g, h)**. Data are presented as mean ± SEM. Cells were enumerated on 10–15 ROIs per section and 3 sections per sample (n=6 for the anterior puncture group and n=4 for the sham group). *, $p<0.05$, student t-test. Scale bar=50 μm.

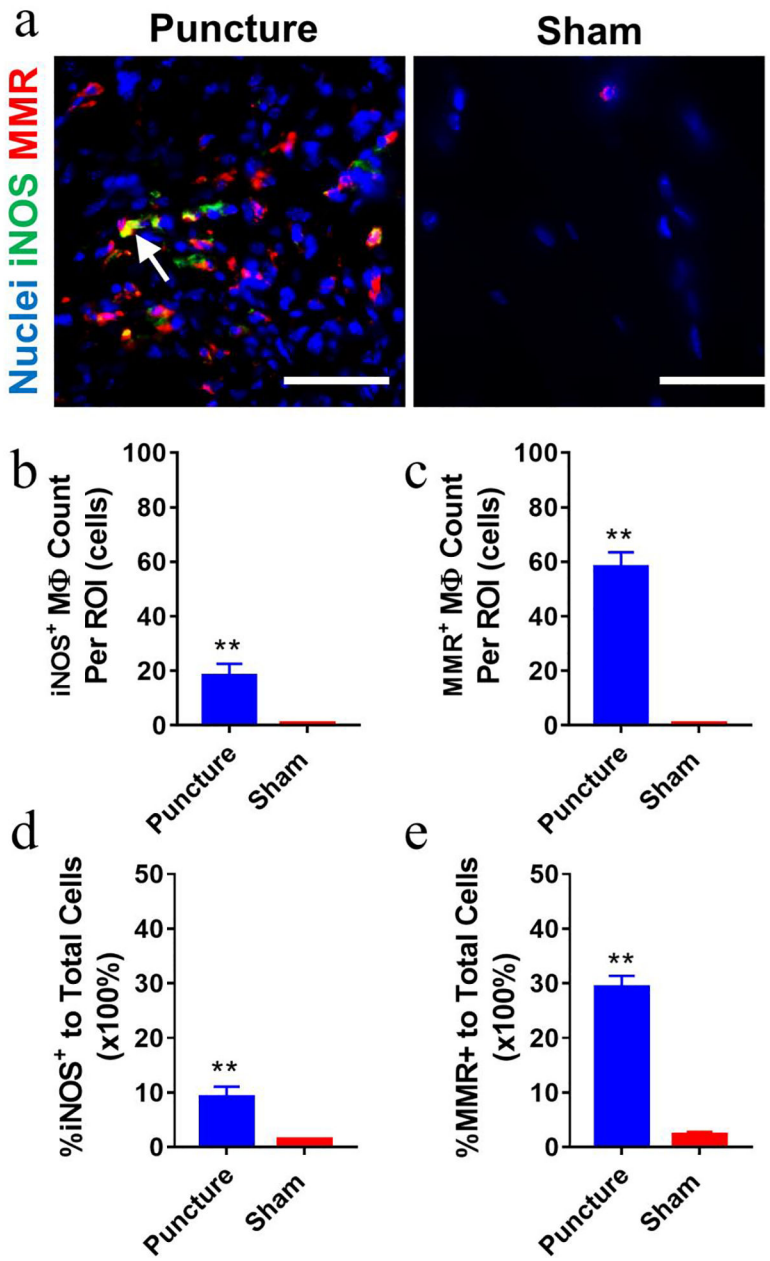

Figure 6. Both M1 and M2-like macrophages were detected in mouse inflammatory infiltration tissues at disc hernia on POD 7.

(a) Representative fluorescence images showed increased iNOS$^+$ and MMR$^+$ macrophages in dissected infiltration tissues of the puncture group compared to the sham. White arrow, iNOS$^+$MMR$^+$. Disc puncture groups showed more iNOS$^+$ **(b, d)** and MMR$^+$ **(c, e)** macrophages compared to the sham group. Data are presented as mean ± SEM. Cells were enumerated on 10–15 ROIs per section and 3 sections per sample (n=6 for anterior puncture group and n=4 for sham group). *, $p<0.05$, student t-test. Scale bar=50 μm.

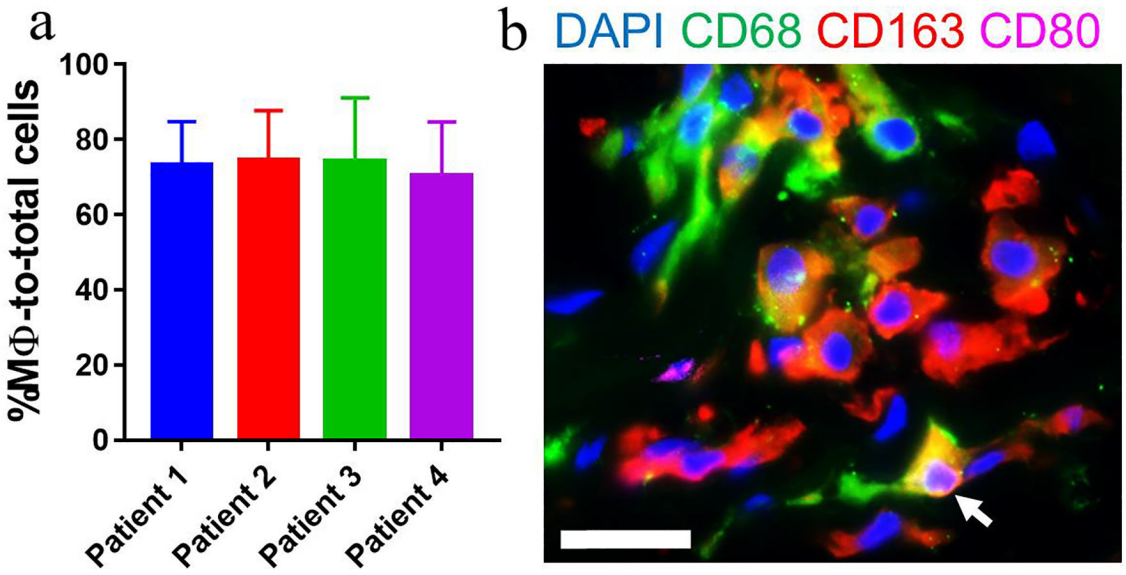

Figure 7. Macrophages were the most abundant cells in human inflammatory disc tissues from patients subjected to discectomy.

(a) Immunofluorescence staining detected abundant $CD68^+$ macrophages with a large number of $CD163^+$ and a small proportion of $CD80^+$ macrophages. **(b)** Quantitative analysis revealed that macrophages accounted for 74.49% ± 3.39% (mean ± SEM, n=4) of total infiltrated cells. Note: the regions containing disc tissue were detectable by autofluorescence and excluded for analysis. Cells were enumerated on 3–5 ROIs per section and 3 sections per sample (n=4). Scale bar=25 μm.

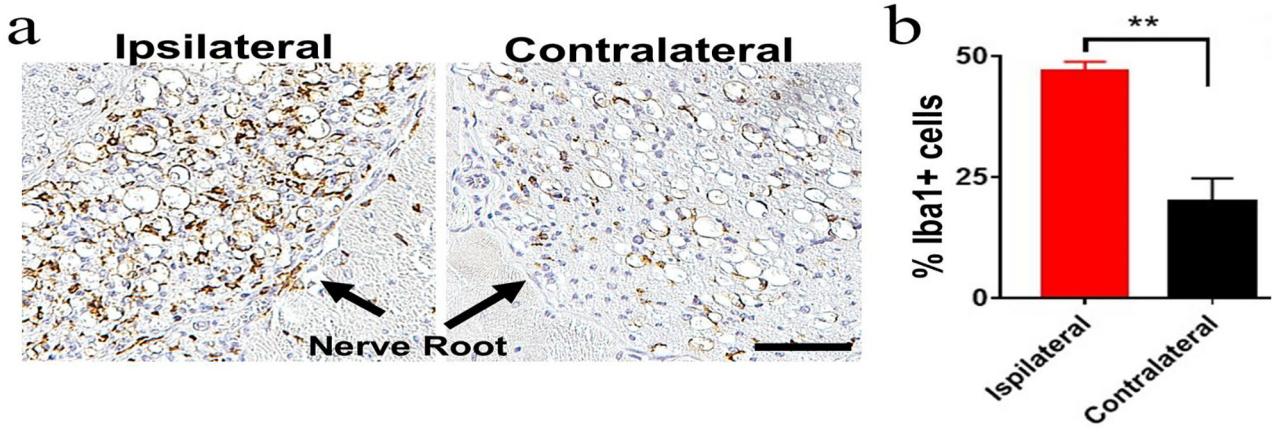

Figure 8. Lateral disc puncture with nerve exposure induced increased Iba1^{+} macrophages/ microglia in the ipsilateral spinal nerves.

(**a**) Immunostaining of axial spine sections showed abundant Iba1^{+} macrophages in the ipsilateral nervescompared to the contralateral nerve on POD 7. Black arrows point to nerves. Scale bar=50 μm. **(b)** Quantitative analysis showed more than a 2-fold increase in Iba1+ cells in the ipsilateral nerve vs. the contralateral side. ** $p<0.01$, $n=3$ per group, unpaired t-test.